Autonomous Multirobot Navigation and Cooperative Mapping in Partially Unknown Environments

Hongyu Xie, *Member, IEEE*, Dong Zhang, *Member, IEEE*, Xiaobo Hu, MengChu Zhou, *Fellow, IEEE*, and Zhengcai Cao, *Senior Member, IEEE*

***Abstract*— To perform collaborative exploration tasks in outdoor environments, multirobot systems require effective task planning and high-precision colocalization. However, there are many challenges in real-world environments, such as unavailable navigation maps and unpredictable obstacles. In this article, we present a system architecture for autonomous multirobot navigation and cooperative simultaneous localization and mapping (SLAM). To enable accurate and efficient multiagent navigation, this work proposes a hierarchical multirobot path planning pipeline involving two tasks, i.e., global multirobot planning and local navigation. The first task is formulated into a min-max k-Chinese postman problem and solved by a genetic algorithm (GA). The second task is transformed into the autonomous collision-free movement of each robot and solved by a reinforcement learning method. To improve the flexibility of cooperative mapping in unknown outdoor environments, this work proposes an online multirobot light detection and ranging (LiDAR) SLAM system, which can flexibly select heterogeneous robots equipped with different sensor combinations. Under the condition of no prior navigation map, this work realizes multirobot cooperative environmental exploration and reconstruction. The proposed system architecture is tested and validated via real-world experiments and some public datasets. Experimental results exhibit the superior performance of the proposed method concerning accuracy, stability, and data efficiency.**

***Index Terms*— Distributed robot systems, light detection and ranging (LiDAR) simultaneous localization and mapping (SLAM), multirobot systems, navigation, path planning.**

I. Introduction

THE unpredictable and unstructured nature of an unknown outdoor environment makes it difficult to design a single robot that can work efficiently and adapts to various terrains. Therefore, multirobot systems have been developed. Through task assignment and data interactions among robots, they can work together to accomplish some time-critical missions, such as search and rescue [1], manufacturing [2], and military tasks [3]. Practical collaborative path planning and robust data association are pivotal technologies essential for facilitating the collaboration of multiple autonomous robots. However, real-world scenarios present enormous challenges, encompassing the absence of prior navigation maps for exploration, presence of unknown obstacles, and deployment of heterogeneous robots equipped with different types of sensors, all of which make accurate interrobot loop closure detection and trajectory estimates difficult. These problems become the factors that negatively impact autonomous multirobot navigation in unknown or partially unknown environments.

Since navigation maps are not always available, traditional map-based path planning methods [4], [5] become infeasible. For multiple robots to cooperatively and autonomously complete an exploration task, a common practice is to add an external localization infrastructure, e.g., global positioning systems (GPSs), georeferenced market, ultrawideband (UWB) [6], and radio frequency identification (RFID) system [7]. However, an external infrastructure is not always reliable. When a robot moves under a tall building or a tree, GPS is not available. The lay georeferenced market or RFID is impractical for emergency tasks. Another attempt is to use simultaneous localization and mapping (SLAM) methods to explore and reconstruct unknown or partially unknown environments [8], [9], [10]. However, SLAM methods require human-controlled robots to generate environmental maps. In practice, satellite maps are usually available. SLAM can be used to provide accurate robot local position and generate a global map for large-scale navigation. Therefore, taking a satellite map as prior knowledge and using cooperative SLAM technology to locate robots should improve the ability of multirobot systems to work autonomously in partially unknown environments.

Single-robot SLAM approaches have been widely researched and many excellent solutions have emerged [11], [12], [13], [14], [15]. Yet, multirobot SLAM is still challenging. Robots need to move to the same position and complete loop detection based on similar environmental observations. Compared with single-robot SLAM, multirobot SLAM is prone to fail due to incorrect data association. As the scope of exploration increases, the time required for interrobot loop closures increases dramatically. Although

Manuscript received 25 July 2023; revised 16 September 2023; accepted 29 September 2023. Date of publication 6 November 2023; date of current version 15 November 2023. This work was supported in part by the National Natural Science Foundation of China under Grant 92148202 and Grant 52175002, in part by the National Key Research and Development Program of China under Grant 2020YFB1313300, in part by the Fundo para o Desenvolvimento das Ciencias e da Tecnologia (FDCT) under Grant 0047/2021/A1, and in part by the Beijing Natural Science Foundation under Grant L223019. The Associate Editor coordinating the review process was Dr. Yan Zhuang. *(Corresponding authors: MengChu Zhou; Zhengcai Cao.)*

Hongyu Xie, Dong Zhang, Xiaobo Hu, and Zhengcai Cao are with the College of Information Science and Technology, Beijing University of Chemical Technology, Beijing 100029, China (e-mail: iexiehongyu@163.com; zhangdong7734@163.com; heyhxb@163.com; caozc@buct.edu.cn).

MengChu Zhou is with the Macao Institute of Systems Engineering and Collaborative Laboratory for Intelligent Science and Systems, Macau University of Science and Technology, Macao 999078, China, and also with the Department of Electrical and Computer Engineering, New Jersey Institute of Technology, Newark, NJ 07102 USA (e-mail: zhou@njit.edu).

Digital Object Identifier 10.1109/TIM.2023.3327469

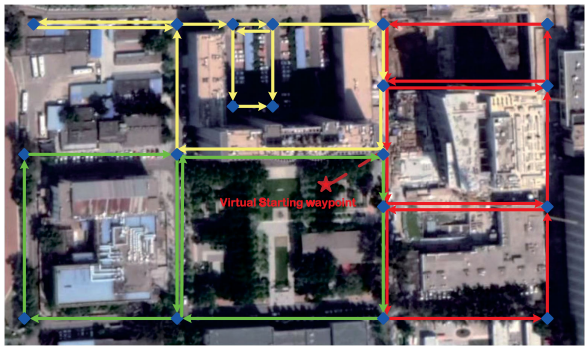

(a)

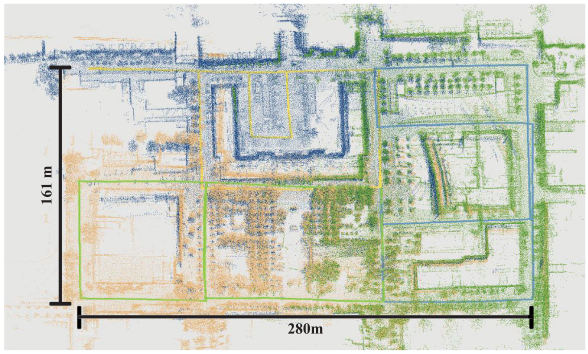

(b)

Fig. 1. Experimental scenario and performance of the proposed multirobot system. (a) Satellite map and GPS data of waypoints are provided as input. (b) Submaps and estimated robot trajectories of robots are represented in the global map in different colors as output.

this topic has received considerable attention [16], [17], multirobot SLAM methods for different sensor suites are lacking. In large-scale unstructured scenarios, different types of robots are suitable for different terrains. Different types of robots have different load capacity and computing power, and the types of sensors equipped are different. Therefore, multirobot systems that can flexibly select heterogeneous robots equipped with different sensor suites are necessary for outdoor mapping.

In this work, we aim to utilize a robot team to cooperatively explore an unstructured outdoor environment. A novel multirobot system architecture is proposed that focuses on two issues: 1) multirobot path planning and end-to-end collision-free navigation in partially unknown environments and 2) online LiDAR-based cooperative localization and mapping. As shown in Fig. 1, the longitude and latitude of global interest points are known. The edges on the graph represent the connectivity between pairs of waypoints. By using the priori, we arrange robots to traverse all edges on the satellite map to generate a global map.

The new contributions this work aims to make are as follows.

1) For the first time, this work formulates a multirobot path planning task into a min-max k-Chinese Postman problem (MKCP). A hierarchical multirobot path planning pipeline is developed to solve it.
2) This work proposes an online multirobot LiDAR-based SLAM system that can select heterogeneous robots and sensor combinations to accomplish cooperative localization and mapping.
3) The proposed method and system architecture are tested and verified by physical experiments and public datasets experiments on KITTI [18] and M2DGR [19].

The rest of this article is organized as follows. Section II provides a review of multirobot path planning and cooperative localization and mapping. Section III describes the proposed system architecture and its tasks. Section IV provides the experimental results. Section V concludes this article with future work indicated.

II. Related Work

A. Multirobot Path Planning

Multirobot path planning is one of the most active research topics in robotics. Most existing algorithms rely on ideal assumptions. For example, under the assumption of a prior navigation map and accurate robot localization, map-based methods [20], [21] can generate the optimal path of a robot by adjusting its motion. To relax the prior map assumption, adding an external localization infrastructure is often needed. However, doing so is expensive and not always reliable. Another attempt is to use SLAM-based methods. Burri et al. [22] construct a globally consistent map for global planning by using visual-based SLAM, and use visual-inertial odometry for local localization in unknown environments. However, it can only be applied to a single robotic navigation task and requires a manually operated flight to generate the initial map. To make full use of environmental information at the beginning stage, Dong et al. [23] extract a set of task viewpoints based on a partially scanned scene, and assign them to robots to cooperatively explore an environment. However, this method is not suitable for outdoor exploration. It is difficult to find closed paths in large-scale outdoor environments, and visual-based localization methods often fail due to motion blur or missing environmental textures [24]. To explore outdoor environments, Bartolomei et al. [25] select some global interest points as the priori. Then, they employ a rapidly exploring random tree method [26] to optimize the path lengths of multi-UAV missions and use a voxblox map for local obstacle avoidance. In contrast to the mentioned work, we formulate a global planning problem into an optimization problem on a graph, which is converted from prior satellite maps. Then, an end-to-end collision-free robot navigation method is performed without building a navigation map. The local position for navigation is obtained by single-robot LiDAR-based odometry.

Thanks to the development of deep learning and deep reinforcement learning, more and more researchers focus on end-to-end navigation methods in unknown environments. Actor-Critic (A-C) series algorithms [27] are proposed and have solved a continuous action problem. Deep deterministic policy gradients (DDPGs) algorithm [28] combines an A-C architecture and deep Q network algorithm [29] to make the training process more stable. Soft actor critic (SAC) algorithm [30] is not only driven by reward, but also uses the entropy output of an actor as the parameter to drive network update, which makes the agent have broader exploration ability

TABLE I
SUMMARY OF THE MOST REPRESENTATIVE MULTIROBOT SLAM FRAMEWORKS, IN CHRONOLOGICAL ORDER

Methods	Sensors	Agents	Odometry agnostic	Data interaction	Data association	Navigation	Open source
DSLAM [31]	Stereo	Datasets		Decentralized	NetVLAD descriptor [32]		[33]
COVINS [34]	Mono, IMU	UAVs		Centralized	Bag-of-words		[35]
[25]	Stereo, IMU, GPS	UAVs		Centralized	Bag-of-words	✓	[36]
DiSCo-SLAM [16]	LiDAR, IMU	UGVs	✓	Decentralized	Scan Context descriptor [37]		[38]
LAMP 2.0 [39]	LiDAR	UGVs	✓	Centralized	Flexible selection		[40]
Swarm-SLAM [41]	Stereo, RGB-D, LiDAR	UGVs	✓	Decentralized	Scan Context / CosPlace		[42]
DCL-SLAM [43]	LiDAR, IMU	UGVs	✓	Decentralized	LiDAR-Iris descriptor [44]		[45]
RDC-SLAM [17]	LiDAR	UGVs		Decentralized	DELIGHT descriptor		-
Ours	LiDAR, IMU, GPS	UGVs	✓	Decentralized	Scan Context descriptor + Geometric constraint	✓	-

Stereo, mono, and RGB-D respectively refer to stereo, monocular, and RGB-D cameras.

and faster training speed. These learning-based methods can convert environmental information into a robot's executable actions. They are widely used in indoor low-speed robot navigation tasks. However, in outdoor scenarios, the variety of obstacles is richer and their movement is more complex. Dynamic obstacles, such as animals, may move irregularly. Static obstacles such as curbs and flower beds seem too low in their height to be classified as obstacles by LiDAR scanning. Considering these limitations, this work develops an end-to-end navigation method. A ground segmentation method is applied as preprocessing, such that a robot plans its motion just between two waypoints without collisions.

B. Multirobot Cooperative Localization and Mapping

SLAM involves simultaneously estimating the state of a robot equipped with onboard sensors and building environmental maps [46]. Since a multirobot SLAM system can transmit information among robots and generate a consistent global map, it can improve the efficiency of exploration tasks over a single robot. Table I lists representative multirobot SLAM systems and their main data interaction and association techniques.

The most commonly used sensors are LiDAR and visual sensors. Since visual sensors can obtain abundant environmental geometrical and texture resources, some multirobot visual-based SLAM methods have emerged [25], [31], [34]. However, visual sensors are sensitive to illumination and texture changes in an environment. It is not suitable for large-scale outdoor environmental reconstruction. Since LiDAR can only obtain sparse environmental geometrical structures, the application of checking interrobot associations from LiDAR scans for online multirobot SLAM systems is limited.

To overcome the interrobot association limitation, there are two main attempts. One is to utilize UWB [47] or GPS to provide a global uniform coordinate system for each robot. In practice, we cannot guarantee the availability of data provided by such sensors. The other is to use 3-D point cloud descriptors to construct correlation for interrobot scans [48]. Huang et al. [16] propose a distributed multirobot SLAM. Their method provides stable localization results by searching for interrobot loop closures under unknown initial conditions. Xie et al. [17] propose a descriptor-based multirobot SLAM method and design a communication protocol to facilitate data association among robots. As running time increases, the descriptor matching time increases, which makes it difficult to guarantee the real-time performance of SLAM. In addition, most multirobot SLAM methods [17], [31], [34] do not consider the different sensor platforms carried by heterogeneous robots and cannot be used to navigate.

Under the condition of ensuring its data availability, this article uses scan context descriptor [37] and GPS data for data association. A two-stage approach is employed to detect interrobot loop closures: 1) GPS data are used for initially judging whether the distance among robots is smaller than the threshold we set and 2) 3-D point cloud descriptor matching is utilized to recognize loops further.

III. SYSTEM ARCHITECTURE

The proposed multirobot system architecture is depicted in Fig. 2. A satellite map is provided as a priori, and a hierarchical planning pipeline is proposed for autonomous multirobot navigation. Heterogeneous robots equipped with different sensor combinations are flexibly selected to perform environmental exploration and mapping tasks. Each robot runs LiDAR-based SLAM for building a submap and performing local collision-free navigation. Since heterogeneous robots are flexibly selected, we can adapt tightly coupled LiDAR inertial odometry via smoothing and mapping (LIO-SAM) [11], LiDAR odometry and mapping (LOAM) [13], and lightweight and ground-optimized LOAM (LeGO-LOAM) [12] to the proposed multirobot system. To find interrobot loop closures more efficiently, we develop an interrobot loop detection method combining GPS and Scan Context 3-D LiDAR descriptors. In order to consistently estimate the global states of all robots, we utilize pose graph optimization to refine robot poses, leveraging the constraints imposed by interrobot loop associations.

A. Prior Information Preprocessing

Given a satellite map of an outdoor environment as a priori, we drive K robots, to cooperatively explore the environment

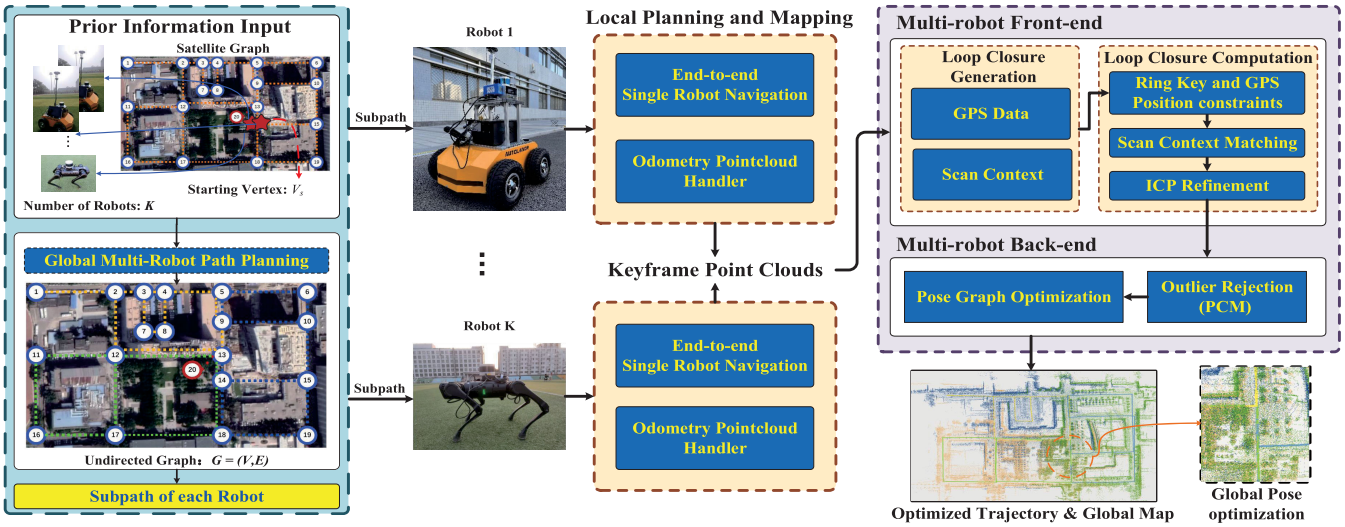

Fig. 2. Structure of our multirobot system. A satellite map is given as a priori. The road connectivity information is used for dividing the working paths. Each robot builds a submap along its planned path. Finally, a global map is generated online by fusing submaps. ICP: iterative closest point method for scan-matching [49]. PCM: the pairwise consistent measurement set maximization method [50].

and reconstruct an environmental structure. Global interest points with their longitude and latitude, and edges connecting these points provide important waypoints and topology information for a multirobot system.

As shown in Fig. 2, graph $G = (V, E)$ is converted from a satellite map. $V = \{v_1, \ldots, v_n\}$ presents a set of n global interest points. $E = \{e_1, \ldots, e_m\}$ presents a set of m paths, and contains all feasible paths among all waypoints in G. In this article, the waypoints are selected by sampling the nodes of the road topology and some waypoints connecting to straight edges. The edges are assumed to be undirected. Each edge has a length $\overleftrightarrow{e_j}$, which can be computed from a given satellite map. The deflection angle a and distance d between two waypoints are calculated in a plane coordinate system

$$\begin{cases} a = \sin^2(\Delta\phi/2) + \cos\phi_1 \cos(\phi_2) \sin^2(\Delta\lambda/2) \\ d = 2R \arctan\left(\sqrt{a}, \sqrt{(1-a)}\right) \end{cases} \tag{1}$$

where $\Delta\phi$ and $\Delta\lambda$ represent the latitude and longitude distance between two waypoints, respectively. R represents the radius (mean radius = 6371 km) of the Earth. The latitude and longitude of a robot are given initially.

B. Autonomous Multirobot Navigation

To achieve effective multirobot collaborative exploration in partially unknown outdoor scenarios, a multirobot path planning task is executed hierarchically with two subtasks: effective global multirobot path planning, and robust local collision-free navigation task.

1) Global Multirobot Path Planning: To maximize the mapping quality while minimizing the scanning effort of all robots, we formulate a global multirobot path planning problem to a well-known MKCP, which is described in [51]. This problem is a kind of graph traversal problem, which can be described as follows: each of K robots finds the shortest closed path in a connected undirected graph G, and the subpaths $\{g_1, g_2, \ldots, g_K\}$ of all robots need to pass through all edges at least once.

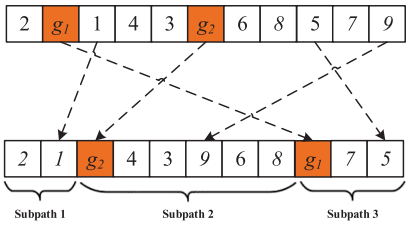

Fig. 3. Process of chromosome and route splitting. There are ten edges in the undirected graph and three robots are used for cooperative environment exploration.

In our work, each robot starts from a given starting waypoint, completes its road exploration, and returns to its starting waypoint. This work aims to visit all edges of an undirected graph at least once. The goal of global multirobot path planning is to minimize the length of the longest subpath $\hat{g}$ and length differences among all subpaths. Let x_{ij} $(i = 1, 2, \ldots, K; j = 1, 2, \ldots, m)$ represent the traversal time of edge e_j in subgraph g_i. The objective function of this problem is

$$\min \max \sum_{j=1}^{m} x_{ij} \overleftrightarrow{e_j}. \tag{2}$$

Since this problem is nondeterministic polynomial-time hard (NP-hard), its possible solution space is too large to search for the optimal solution in a reasonable time. Thus, we develop a genetic algorithm (GA) to solve it. GA is a meta-heuristic algorithm for optimization and search problems [52]. It iteratively optimizes the solution to the problem via genetic mutation, natural selection, and crossover observed in a process of biological evolution. How to design the genetic representation of a candidate solution and a fitness function are two key issues.

In this work, a chromosome is designed as a string of numbers (as shown in Fig. 3). Different from [53], its length

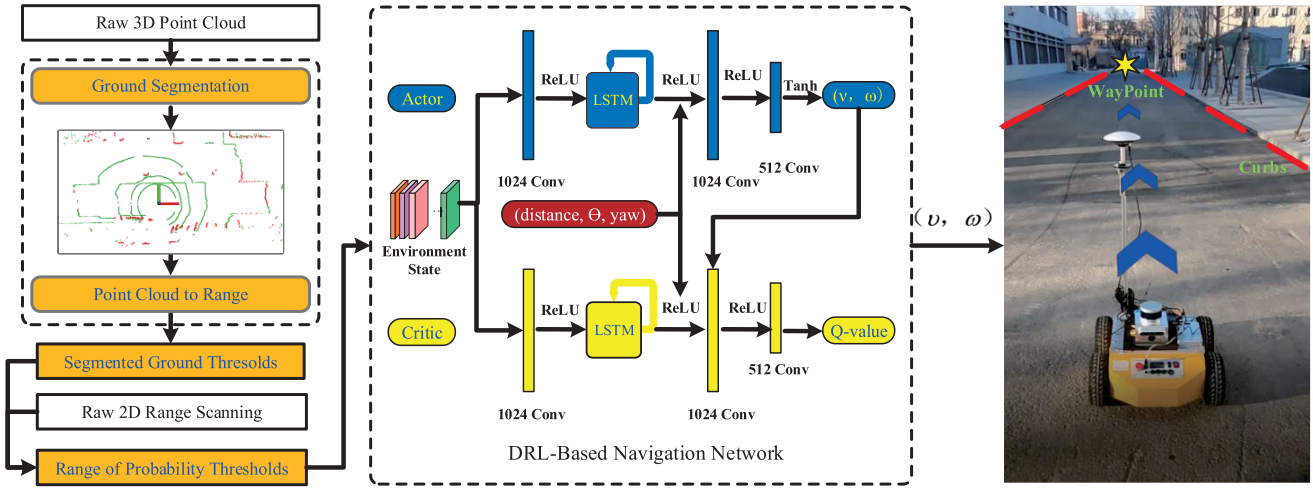

Fig. 4. Process of autonomous collision-free movement. The raw 3-D point clouds and 2-D range scanning of the LiDAR sensor are used as input, and the output is the motion plan of the robot, including linear velocity and angular velocity.

is set to $L = m + K - 2$, which denotes the number of m edges and K robots. Assuming that K robots can go through the same starting edge e_m, e_1 to e_{m-1} represent the remaining edges. $K-1$ virtual numbers are used to divide K robot subpaths. Such gene coding makes it easy for crossover and mutation operators to generate new solutions. The fitness function in this work is set as the weighted sum of the total length of all robot subpaths and the longest subpath's length

$$F = \lambda K \left\{ \max \sum_{j=1}^{m} x_{ij} w(e_j) \right\} + \beta \sum_{i=1}^{K} \sum_{j=1}^{m} x_{ij} w(e_j) \quad (3)$$

where λ and β represent the weights of the generated total path's length and the longest subpath's length, respectively. In this article, the λ and β are set to 0.5 to get the shortest longest path and the shortest total path. When evaluating chromosomes, we use two waypoints to represent an edge. The starting waypoint may correspond to several lines. To avoid ambiguity of an initial waypoint, we add a virtual edge in the graph, which only contains a dummy waypoint and the starting waypoint. This virtual edge is used to ensure the starting waypoint is unique. We use an adjacency matrix and Floyd algorithm to calculate the shortest path from one waypoint to another. The shortest path from one edge to another is converted to the shortest path from one waypoint to another. The selected individual chromosomes are split and exchanged via an ordered crossover (OX) to form the next-generation solution.

2) Local Collision-Free Navigation: The environmental undirected graph-based planning partitions multirobot path planning tasks into groups. The local position of each robot is optimized by LiDAR-based odometry. Given the direction and distance from the current waypoint to the target one, each robot focuses on its collision-free navigation task between two waypoints. In this work, we develop a deep reinforcement learning (DRL)-based method with ground segmentation, as shown in Fig. 4. We adopt a navigation network in [54], which is based on long short-term memory (LSTM) and DDPG, and essentially an A-C strategy algorithm. The 360° laser scanning

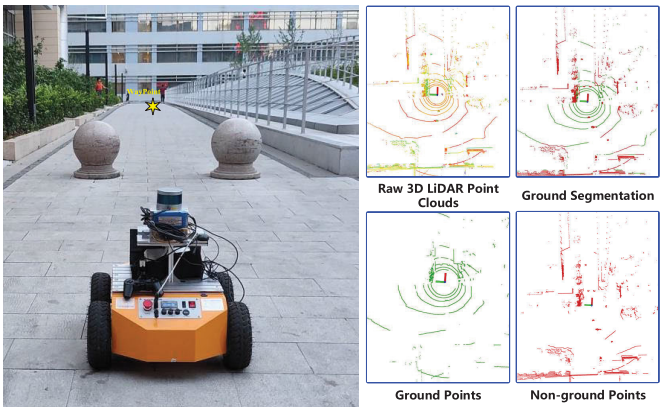

Fig. 5. Ground segmentation is performed on the raw 3-D LiDAR point cloud, the green and red points denote the ground points and nonground points.

data, yaw angle, and the relative position between the current waypoint and the target one are taken as input. An actor network is used to output actions (linear velocity ν and angular velocity ω that the robot needs to perform). A critic network is used to estimate the Q value of the actor's output actions. Until the distance between a robot and its target waypoint is less than 0.2 m, we consider it as reaching the target waypoint. Since the actually arrived position does not completely coincide with the waypoint generated based on a satellite map, we use the estimated global pose of a robot and recalculate the relative position between the current position of a robot and its target waypoint.

In addition to high obstacles such as pedestrians, vehicles, and trees, there are also some low obstacles, such as curbs and flower beds. It is difficult to obtain complete environmental data through 2-D LiDAR scanning. To avoid these obstacles, this work adopts a ground segmentation method [55] for feasible domain segmentation processing of 3-D LiDAR point clouds. The raw point cloud captured by a Velodyne VLP-16 LiDAR sensor is taken as an example. As shown in Fig. 5, the ground segmentation result shows that low and dynamic

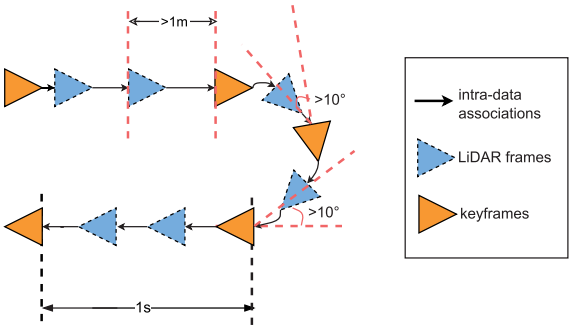

Fig. 6. Demonstration of keyframe selection.

obstacles have been segmented well. To compensate for the underfitting of ground segmentation, laser scans approximately parallel to the ground are combined with the generated ground segmentation results.

C. Single Robot Odometry and Keyframe Selection

To estimate a single robot's motion and keep a 3-D map along its preplanned path, each robot runs real-time odometry onboard. Our proposed framework supports different kinds of LiDAR-based odometry systems on robots. Among them, the inclusion of an inertial measurement unit (IMU) provides high frequency and accurate inertial measurements, free from any outliers. GPS offers precise positioning in areas with reliable satellite visibility. The selection of the odometry system depends primarily on the onboard sensors and computing resources of robots. In our implementation, we use the LiDAR-based odometry system from LIO-SAM [11], in the condition of a robot equipped with a combined sensor suite of LiDAR, IMU, and GPS, since LIO-SAM is one of the highly accurate LiDAR inertial odometry systems. LeGO-LOAM [12] and LOAM [13] are chosen when there is no IMU device, and LeGO-LOAM is chosen if the robot has limited computational capabilities.

For each incoming point cloud, we execute feature extraction and the corresponding feature matching to guarantee the required positioning frequency and accuracy of LiDAR odometry. Meanwhile, the point cloud need to pass to the module to realize interrobot loop detection. To better reduce computational expense and data buffer, we apply a keyframe selection method similar to [11]. Only the point cloud at the keyframe will send to the Multirobot front-end module, and determine whether there has an interrobot loop closure. As illustrated in Fig. 6, a frame is identified as a keyframe when one of the following two conditions is met.

1) The pose of the robot changes more than 1 m or 0.2 rad.
2) More than 1 s has passed since the last keyframe was added.

Condition (a) ensures enough similar structure between keyframes, while (b) takes effect in the absence of keyframes caused by long-term low-speed movement.

D. Data Association and Pose Optimization

The multirobot collaborative mapping module in our framework operates persistently at each robot's end while executing the individual robot's SLAM process. Algorithm 1 realizes the process of data association and optimization in multirobot cooperative mapping.

Algorithm 1 Interrobot Relative Pose Estimation

Input: Point cloud P_{id} from robot id
Robot pose sequence T_{id} of robot id
Output: Robot global pose sequence T

#Extract descriptor feature and construct KD tree
$SC_{id} \leftarrow ExtractScanContext(P_{id})$
$RK_{id} \leftarrow ExtractRingKey(SC_{id})$
#Search candidate interrobot loop closure
$X^*_{sc_{id}} \leftarrow KNNSearch(RK_{id})$
foreach $x_{sc_{id}}$ **do**
  $D_{GPS} \leftarrow BetweenGPS(x^C_{sc_{id}}, x^M_{sc_{id}})$
  $D_{SC} \leftarrow BetweenSC(x^C_{sc_{id}}, x^M_{sc_{id}})$
  if $D_{SC} \leq D_s$, $D_{GPS} \leq D_g$ **then**
    CalculateICPFitnessScore($x^C_{sc_{id}}, x^M_{sc_{id}}$)
  end
end
#False interrobot constraints removal
$X_{sc_{id}} \leftarrow PCM(X^*_{sc_{id}})$
#Interrobot constraints optimization
$T \leftarrow PoseGraphOptimize()$
$X_{pose_{id}} \leftarrow KNNSearch(T_{id})$
$T \leftarrow PoseGraphOptimize()$
return T

1) Interrobot Loop Closure: To explore interrobot alternative matches, scan context and GPS data (if a robot has a GPS receiver) are utilized to identify potential data association. Our system exchanges data in a distributed manner. Each robot receives point clouds and GPS data at the keyframes of other robots. We assign a unique letter to each robot to attribute which robot has created the keyframe. Scan context is used as the global descriptor. It is composed of height information of the 3-D scans in divided grid cells. Ring key is an N-dimensional vector extracted from scan context. For each incoming point cloud, we encode it into scan context and generate a ring key for candidate interrobot loop closure search.

The ring key is utilized to construct a K-Dimensional tree (KD tree) for fast search. After finding possible candidates for a loop, a set of pairs, denoted as X^*_{sc}, is obtained. Each pair consists of a current robot frame x^C_{sc} and a matched robot frame x^M_{sc}. We measure the distance D_{GPS} and D_{SC}, representing the spatial distance between two robots and the similarity score between two scan contexts. Once identifying a loop-closure candidate, iterated closest point (ICP) [49] is utilized to compute the relative pose transformation between two robots and obtain fitness values.

2) False Constraint Removal: To further eliminate interrobot mismatches, we use pairwise consistency maximization (PCM) in [50] to find the largest set of consistent loop closures by verifying if pairs of loop closures X^*_{sc} are consistent with others. The following condition is met for a loop closure to

TABLE II
HETEROGENEOUS ROBOTS EQUIPPED WITH DIFFERENT SENSOR COMBINATIONS

Robots	Sensors	Processor
Wheeled Robot 1	1 x Velodyne VLP-16 LiDAR 1 x Ublox ZED-F9P GNSS receiver 1 x Xsens Mti 680 G IMU	Intel i7-10875H CPU 16GB DDR4 RAM
Wheeled Robot 2	1 x Velodyne VLP-16 LiDAR 1 x Ublox ZED-F9P GNSS receiver	Intel i5-8550U CPU 8GB DDR3 RAM
Quadruped Robot 3	1 x Velodyne VLP-16 LiDAR	Intel i5-8550U CPU 8GB DDR3 RAM

be accepted:

$$\left\| \left(z_{\beta_j \beta_l} \cdot x_{\alpha_i \beta_j} \cdot z_{\alpha_i \alpha_k} \right) \cdot {x_{\alpha_k \beta_l}}^{-1} \right\|_2^2 < \varepsilon. \tag{4}$$

$z_{\beta_j \beta_l}$ and $z_{\alpha_i \alpha_k}$ are the pose variations of robot β and robot α between frames j to l and i to k, respectively. $x_{\alpha_i \beta_j}$ and $x_{\alpha_k \beta_l}$ are loop closure measurements between robots β and α. ε is a threshold value set based on an expert's experience.

3) Robot Pose Optimization: We employ pose graph optimization to refine the estimation of individual robot poses in the presence of interrobot loop closure. A pose graph is a structure that consists of interconnected nodes and edges. The nodes within the graph represent the pose of robots, indicated as $\{z_{\alpha_i}, z_{\alpha_k}, \ldots, z_{\beta_j}, z_{\beta_l}, \ldots\}$. The edges, indicated as $\{x_{\alpha_i \beta_j}, x_{\alpha_k \beta_l}, \ldots\}$, represent constraints arising from interrobot loop closure measurements.

To perform pose graph optimization, we initially construct edges in the pose graph based on loop closure identified through descriptor search. Once the initial registration is successful, we conduct an additional interrobot loop closure search within the graph to identify the prior states X_{pose} that exhibit proximity in terms of Euclidean space, and utilize these loop measurements to perform optimization again. In this way, the consistency in the estimation of poses is improved.

IV. EXPERIMENTAL RESULTS

In this section, we verify our multirobot system by testing in some real-world environments and on public datasets. All the methods are executed on a laptop using the robot operating system (ROS) in the Ubuntu platform without parallel computing enabled. The subsequent experiments are performed on multiple computers, including one equipped with an Intel i7-10875H CPU, 16 GB DDR4 RAM, and two with an Intel i5-8550U CPU and 8 GB DDR3 RAM, which takes charge of computation on one single robot.

A. Experimental Setup

The real-world experiments are performed in two different scenarios, referred to as West and East, respectively. All data are collected on the campuses of the Beijing University of Chemical Technology. As shown in Table II, robot 1–3 are equipped with different sensors.

To verify the performance of the proposed system, we conduct four different experiments across various scales, and platforms on two different campuses, respectively. West datasets are collected from a campus of about 20 000 square meters. Based on a satellite map of the West scenario, we use GA to divide the working paths for robot teams with different numbers of robots, and arrange robots to explore this scenario. W1, W2, and W3 are data collected by the number of robots from 1 to 3. In these experiments, the satellite map is formulated into an undirected graph with 26 vertices and 29 edges. The virtual starting waypoint V_{26} is used to ensure that GA has a unique starting waypoint and starting edge. E3 is collected from a campus of about 90 000 square meters. The satellite map of it is formulated into an undirected graph with 20 vertices and 27 edges with the virtual starting waypoint V_{20}. We use GA to divide the working paths of three robots, and arrange them to explore this scenario. In all mentioned experiments, each robot moves along the given subpath, and collects timestamp-aligned LiDAR, IMU, and GPS data. Evo tool [56] is used to quantitatively analyze the accuracy of the proposed multirobot SLAM.

B. Autonomous Multirobot Navigation

Given the prior satellite maps, we formulate a multirobot path planning task into an MKCP. Since its global optimal solution is not available, a single-robot optimal solution generated by the method [57] is used as a reference solution to estimate the quality of solutions generated by GA. After testing, the total path lengths of single-robot obtained by the two methods are equal.

To extend GA to multiple robots, we use one or three robots as an example: after several iterations, GA can gradually obtain the optimal path of a single robot. As shown in Fig. 7, GA can iteratively optimize the subpaths of robots, and the fitness increases as the length of the optimal path decrease. It shows that GA is feasible for solving a multirobot path planning problem. The division of the workspace and the length of each robot subpath are relatively balanced.

To discuss the relationship between the mapping efficiency and the number of robots, we calculate the changes in the total path length, longest subpath length, and average path length of robots when using the number of robots varying from 1 to 10. Under the assumption that all robots pass through the same point, the efficiency of mapping does not always improve. As shown in Fig. 8, when the number of robots reaches a certain value, the longest subpath length determines that the mapping efficiency no longer increases. The length of the longest subpath is the minimum length of the loop where a robot starts from the starting waypoint, reaches the farthest waypoint, and then returns to the starting waypoint.

C. Local and Global Pose Estimation and Mapping

1) Pose Estimation and Mapping: Along the path planned by completing a navigation task, each robot performs pose estimation and map generation in its local coordinate system. Based on the proposed distributed multirobot cooperative mapping system, each robot performs map fusion and maintains a

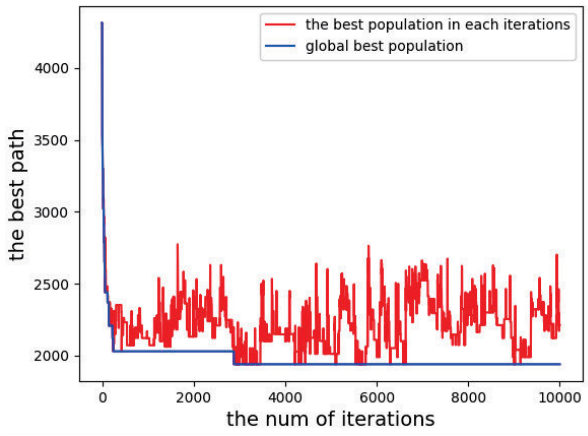

(a)

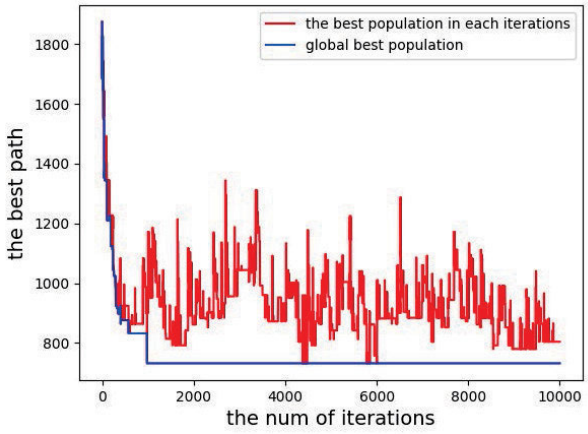

(b)

Fig. 7. Change of global optimal solution in (a) E1 and (b) W3.

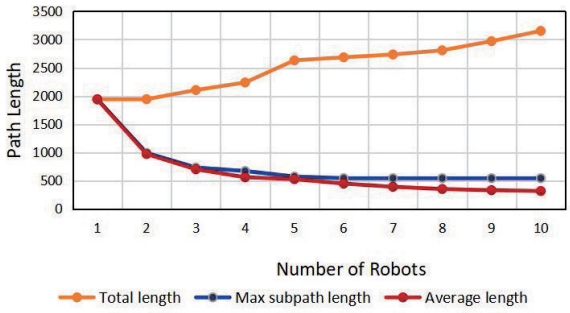

Fig. 8. Total length of subpaths and the longest subpath length change (m) with the number of robots.

global map. To verify the validity and accuracy of the proposed system, we design some experiments on W1–W3 and E3 datasets. The generated global maps and trajectories of each robot in the global coordinate systems are shown in Fig. 9. As expected, the fused maps achieve well global consistency. To test the localization accuracy of each robot, we calculate the end-to-end relative translation error by making each robot returns to the starting waypoint. E3-RX and W3-RX ($X \in \{1, 2, 3\}$) represent the data collected by the ith robot on E3 and W3 datasets. The result is shown in Table III.

To quantitatively analyze the mapping result, we use absolute trajectory error (ATE) as an evaluation metric. To ensure

TABLE III
END-TO-END TRANSLATION ERROR (METERS)

Scenario	W3-R1	W3-R2	W3-R3	E3-R1	E3-R2	E3-R3
Dist (m)	371	421	369	719	775	708
Error (m)	0.16	0.12	0.19	0.07	0.09	0.15

TABLE IV
ATE WITH RESPECT TO GPS

Dataset	PL-R1	PL-R2	PL-R3
Duration (s)	99	187	318
Dist (m)	83.7	131.6	216.4
RMSE (m)	0.263	0.485	0.480

our global navigation satellite system-real-time kinematic (GNSS-RTK) suite outputs available ground truth free from buildings and trees affecting the signal, we record a three-robot dataset in a parking lot as the supplementary, referred to as the PL dataset. PL-R1, PL-R2, and PL-R3 represent the data collected by three robots R1-R3, respectively. PL-R1 is collected by a robot equipped with LiDAR, IMU, and GPS; PL-R2 a robot with LiDAR and GPS; and PL-R3 a robot with LiDAR. Before performing map fusion, each robot estimates state and builds its map in its reference frame. The respective trajectories of each robot and the merged map are shown in Fig. 10. We calculate the ATE for each estimated robot trajectory as shown in Table IV. As expected, the merged map achieves global consistency well under the premise of the estimated pose of each robot being consistent.

2) Communication: Interrobot data exchange necessitates the utilization of communications. Considering the limitations imposed by a communication range, in the testing scenes encompassing W2, W3, and E3, we first send ping messages to ensure that the robots are within the range. In testing scenarios involving short communication distances, such as PL, the longest path traveled by the robot is 200 m, this step is deemed superfluous. To alleviate the burden on communication bandwidth, we do not transmit data for every frame.

D. Evaluation on KITTI and M2DGR Datasets

To assess the efficacy of our multirobot SLAM system, we conduct a comprehensive validation study. We next present the results by using two publicly available datasets configured for testing 3-D LiDAR SLAM, and refer to the datasets as KITTI and M2DGR.

The KITTI dataset is composed of real LiDAR, camera, IMU, and GPS data collected by cars in various road scenes. The M2DGR dataset is collected from campus scenes by a ground robot including LiDAR, camera, IMU, and GPS data. Since both are not designed to validate multirobot systems, we divide each of them into two subsequences. We must ensure that there is an overlap between two subsequences. KITTI is divided into two subsequences, each with a duration of 155 s. It modifies the raw dataset into a synthetic two-robot dataset. M2DGR is divided into two subsequences with

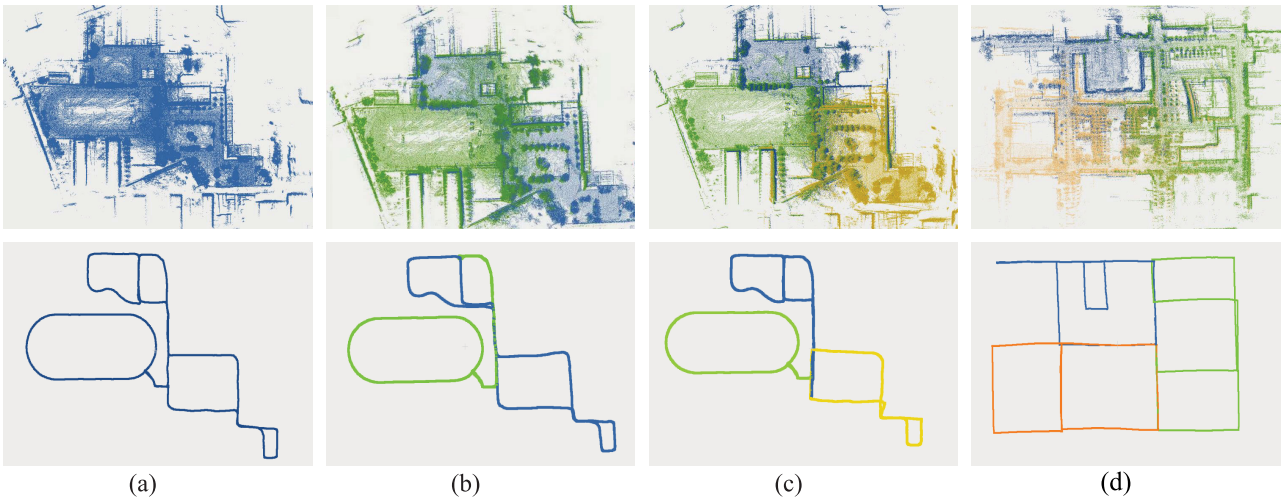

Fig. 9. Global map generated and the trajectories fused on (a) W1, (b) W2, and (c) W3 by one to three robots, and (d) E3 by three robots. The trajectory estimated and map generated by each robot are drawn in different colors.

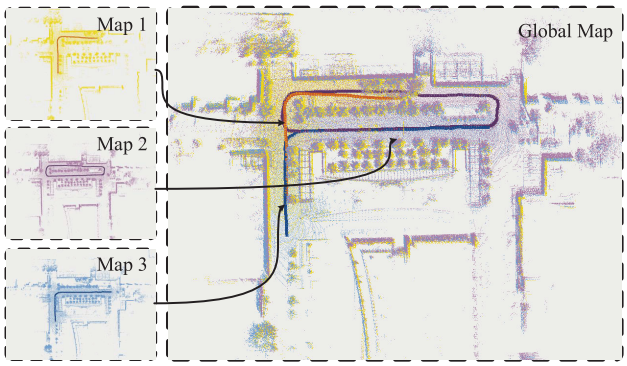

Fig. 10. Demonstration of the proposed multirobot SLAM on parking.

an equal duration of 500 s, and we change the time-stamps to incorporate overlap.

During the evaluation conducted on the dataset, we make the assumption of an unbounded communication range, which facilitates unrestricted message exchange among the robots at any time. Fig. 11 shows the maps and trajectories generated by DiSCo-SLAM and our method. Compared to DiSCo-SLAM, our method exhibits improved consistency in trajectory estimation in the overlapping regions of the paths executed by the two robots. This is especially evident when evaluating our method on the KITTI dataset.

In order to quantitatively evaluate the accuracy of robot trajectory estimation, we use the ATE as a metric. As shown in Table V, the minimum, mean, and root mean square error (RMSE) of ATE are computed to provide statistical insights. The experiments on KITTI and M2DGR verify the effectiveness of our collaborative mapping method in urban road scenarios and open campus environments.

E. Communication and Computational Efficiency

To quantify the data communication size among robots, we count the number of frames and keyframes during the running of multirobot system. To reduce the communication burden, only the data at keyframes is transmitted. The experimental results of tests on the PL dataset are shown in Table VI. The number of keyframes accounts for less than 20% of the total frames, and each keyframe has a data size of less than 200 KB, which can meet the requirements for real-time communication.

The introduction of GPS data used in interrobot loop closures can efficiently reduce the matching time among robots. As shown in Table VII, our system is effective in reducing the number of candidate loops in different scenarios. Fewer candidate loops can reduce the time spent in subsequent steps.

TABLE V
COMPARISON RESULTS OF METRIC ATE (m)

Dataset	Methods	Min (m)	Mean (m)	RMSE (m)
KITTI05	DiSCo-SLAM	0.22	1.53	1.82
	Ours	0.15	1.36	1.61
M2DGR	DiSCo-SLAM	0.19	0.82	0.98
	Ours	0.15	0.81	0.98

TABLE VI
MEAN NETWORK TRAFFIC PER KEYFRAME

Scenario	**PL-R1**	**PL-R2**	**PL-R3**
Frames	987	1872	3309
Keyframes	163	301	576
Feature point cloud(KB)	194	174	133
Robot pose(KB)	<1	<1	<1

TABLE VII
EFFICIENCY IMPROVEMENT THROUGH GPS ASSISTANCE

	Without GPS		GPS Assistance	
	Times (s)	Candidate loop closures	Times (s)	Candidate loop closures
W2	67.6	357	46.7	283
PL	38.0	559	33.3	542

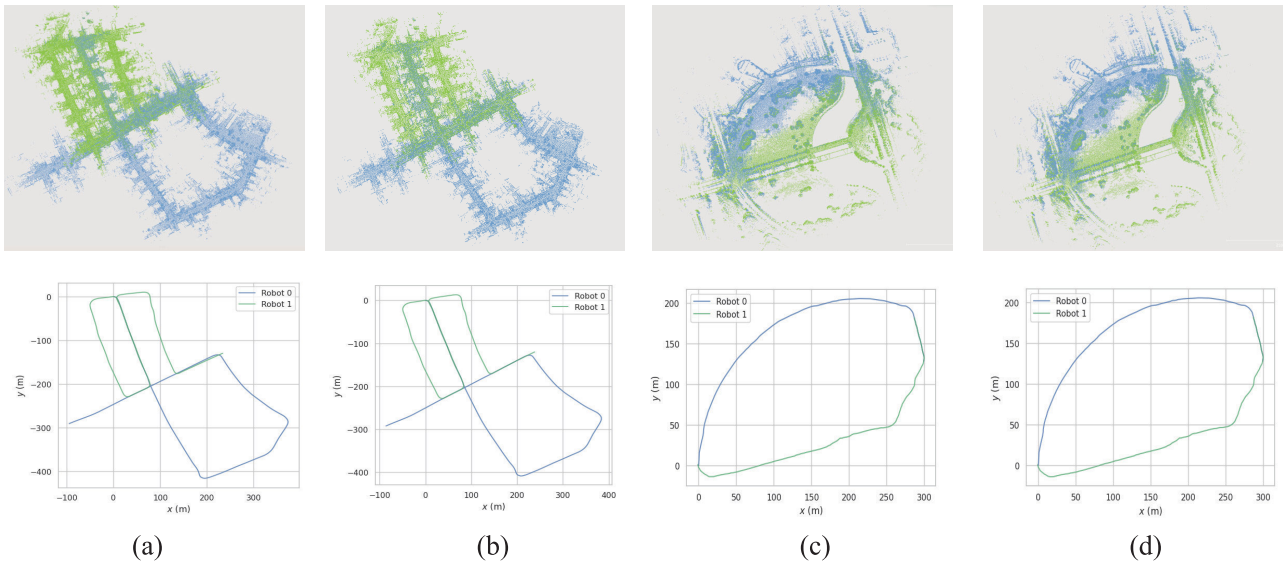

Fig. 11. Global map generated and the trajectories estimated on KITTI05 by (a) DiSCo-SLAM and (b) ours, M2DGR street04 by (c) DiSCo-SLAM and (d) ours.

We accumulate the time spent in loop closure computation and multirobot back-end. Table VII shows that by setting the GPS threshold to 10 m in our system, the matching time is greatly reduced.

V. Conclusion

In this work, we present a novel multirobot system architecture, which is designed for multiple autonomous robots to explore partially unknown environments. This work divides the collaborative exploration task into two main modules: cooperative searching and local maps merging. An undirected graph-based hierarchical navigation strategy is proposed, which can utilize incomplete environmental information. We also improve the interrobot loop closure detection by combining GPS and geometric descriptor information. It can receive information from different heterogeneous robots with different front-end odometry methods, and realize accurate interrobot loop closure detection and trajectory estimates. In addition to verifying the efficiency and accuracy of the proposed system on public datasets, we also verified its effectiveness in real scenarios.

This work focuses on exploring an outdoor environment while building a global map. To make a multirobot system better adapt to environments, an interesting line of research is the online multirobot path planning by considering unreachable points and traffic jams [58].

References

[1] M. J. Schuster, C. Brand, H. Hirschmüller, M. Suppa, and M. Beetz, "Multi-robot 6D graph SLAM connecting decoupled local reference filters," in *Proc. IEEE/RSJ Int. Conf. Intell. Robots Syst. (IROS)*, Sep. 2015, pp. 5093–5100.

[2] C. Eschke, M. K. Heinrich, M. Wahby, and H. Haman, "Self-organized adaptive paths in multirobot manufacturing: Reconfigurable and pattern-independent fibre deployment," in *Proc. IEEE/RSJ Int. Conf. Intell. Robots Syst. (IROS)*, Nov. 2019, pp. 4086–4091.

[3] L. E. Parker, "Distributed intelligence: Overview of the field and its application in multirobot systems," *J. Phys. Agents (JoPha)*, vol. 2, no. 1, pp. 5–14, 2008.

[4] W. Hess, D. Kohler, H. Rapp, and D. Andor, "Real-time loop closure in 2D LiDAR SLAM," in *Proc. IEEE Int. Conf. Robot. Autom. (ICRA)*, May 2016, pp. 1271–1278.

[5] G. Grisetti, C. Stachniss, and W. Burgard, "Improved techniques for grid mapping with Rao-Blackwellized particle filters," *IEEE Trans. Robot.*, vol. 23, no. 1, pp. 34–46, Feb. 2007.

[6] J. Wang, Z. Meng, and L. Wang, "Efficient probabilistic approach to range-only SLAM with a novel likelihood model," *IEEE Trans. Instrum. Meas.*, vol. 70, pp. 1–12, 2021.

[7] J. Wang, Z. Meng, and L. Wang, "A UPF-PS SLAM algorithm for indoor mobile robot with NonGaussian detection model," *IEEE/ASME Trans. Mechatronics*, vol. 27, no. 1, pp. 1–11, Feb. 2022.

[8] J. Ma, K. Zhang, and J. Jiang, "Loop closure detection via locality preserving matching with global consensus," *IEEE/CAA J. Autom. Sinica*, vol. 10, no. 2, pp. 411–426, Feb. 2023.

[9] Z. Gao, J. Qin, S. Wang, and Y. Wang, "Boundary gap based reactive navigation in unknown environments," *IEEE/CAA J. Autom. Sinica*, vol. 8, no. 2, pp. 468–477, Feb. 2021.

[10] H. Zhang, L. Jin, and C. Ye, "An RGB-D camera based visual positioning system for assistive navigation by a robotic navigation aid," *IEEE/CAA J. Autom. Sinica*, vol. 8, no. 8, pp. 1389–1400, Aug. 2021.

[11] T. Shan, B. Englot, D. Meyers, W. Wang, C. Ratti, and D. Rus, "LIO-SAM: Tightly-coupled LiDAR inertial odometry via smoothing and mapping," in *Proc. IEEE/RSJ Int. Conf. Intell. Robots Syst. (IROS)*, Oct. 2020, pp. 5135–5142.

[12] T. Shan and B. Englot, "LeGO-LOAM: Lightweight and ground-optimized LiDAR odometry and mapping on variable terrain," in *Proc. IEEE/RSJ Int. Conf. Intell. Robots Syst. (IROS)*, Oct. 2018, pp. 4758–4765.

[13] J. Zhang and S. Singh, "LOAM: LiDAR odometry and mapping in real-time," *Robot., Sci. Syst.*, vol. 2, no. 9, pp. 1–9, 2014.

[14] G. He, X. Yuan, Y. Zhuang, and H. Hu, "An integrated GNSS/LiDAR-SLAM pose estimation framework for large-scale map building in partially GNSS-denied environments," *IEEE Trans. Instrum. Meas.*, vol. 70, pp. 1–9, 2021.

[15] Y. Pan, X. Xu, X. Ding, S. Huang, Y. Wang, and R. Xiong, "GEM: Online globally consistent dense elevation mapping for unstructured terrain," *IEEE Trans. Instrum. Meas.*, vol. 70, pp. 1–13, 2021.

[16] Y. Huang, T. Shan, F. Chen, and B. Englot, "DiSCo-SLAM: Distributed scan context-enabled multirobot LiDAR SLAM with two-stage global-local graph optimization," *IEEE Robot. Autom. Lett.*, vol. 7, no. 2, pp. 1150–1157, Apr. 2022.

[17] Y. Xie et al., "RDC-SLAM: A real-time distributed cooperative SLAM system based on 3D LiDAR," *IEEE Trans. Intell. Transp. Syst.*, vol. 23, no. 9, pp. 14721–14730, Sep. 2022.

[18] A. Geiger, P. Lenz, and R. Urtasun, "Are we ready for autonomous driving? The KITTI vision benchmark suite," in *Proc. IEEE Conf. Comput. Vis. Pattern Recognit.*, Jun. 2012, pp. 3354–3361.

[19] J. Yin, A. Li, T. Li, W. Yu, and D. Zou, "M2DGR: A multi-sensor and multi-scenario SLAM dataset for ground robots," *IEEE Robot. Autom. Lett.*, vol. 7, no. 2, pp. 2266–2273, Apr. 2022.

[20] Z. Yang and R. Tron, "Multi-agent path planning under observation schedule constraints," in *Proc. IEEE/RSJ Int. Conf. Intell. Robots Syst. (IROS)*, Oct. 2020, pp. 6990–6997.

[21] X. Ji, H. Li, Z. Pan, X. Gao, and C. Tu, "Decentralized, unlabeled multi-agent navigation in obstacle-rich environments using graph neural networks," in *Proc. IEEE/RSJ Int. Conf. Intell. Robots Syst. (IROS)*, Sep. 2021, pp. 8936–8943.

[22] M. Burri, H. Oleynikova, M. W. Achtelik, and R. Siegwart, "Real-time visual-inertial mapping, re-localization and planning onboard MAVs in unknown environments," in *Proc. IEEE/RSJ Int. Conf. Intell. Robots Syst. (IROS)*, Sep. 2015, pp. 1872–1878.

[23] S. Dong et al., "Multi-robot collaborative dense scene reconstruction," *ACM Trans. Graph.*, vol. 38, no. 4, pp. 1–16, Aug. 2019.

[24] H. Xie et al., "Semi-direct multimap SLAM system for real-time sparse 3-D map reconstruction," *IEEE Trans. Instrum. Meas.*, vol. 72, pp. 1–13, 2023, doi: 10.1109/TIM.2023.3240206.

[25] L. Bartolomei, M. Karrer, and M. Chli, "Multi-robot coordination with agent-server architecture for autonomous navigation in partially unknown environments," in *Proc. IEEE/RSJ Int. Conf. Intell. Robots Syst. (IROS)*, Oct. 2020, pp. 1516–1522.

[26] S. Karaman and E. Frazzoli, "Sampling-based algorithms for optimal motion planning," *Int. J. Robot. Res.*, vol. 30, no. 7, pp. 846–894, Jun. 2011.

[27] V. R. Konda and J. N. Tsitsiklis, "OnActor-critic algorithms," *SIAM J. Control Optim.*, vol. 42, no. 4, pp. 1143–1166, Jan. 2003.

[28] T. P. Lillicrap et al., "Continuous control with deep reinforcement learning," 2015, *arXiv:1509.02971*.

[29] V. Mnih et al., "Human-level control through deep reinforcement learning," *Nature*, vol. 518, no. 7540, pp. 529–533, 2015.

[30] T. Haarnoja, A. Zhou, P. Abbeel, and S. Levine, "Soft actor-critic: Off-policy maximum entropy deep reinforcement learning with a stochastic actor," in *Proc. Int. Conf. Mach. Learn.*, 2018, pp. 1861–1870.

[31] T. Cieslewski, S. Choudhary, and D. Scaramuzza, "Data-efficient decentralized visual SLAM," in *Proc. IEEE Int. Conf. Robot. Autom. (ICRA)*, May 2018, pp. 2466–2473.

[32] R. Arandjelovic, P. Gronat, A. Torii, T. Pajdla, and J. Sivic, "NetVLAD: CNN architecture for weakly supervised place recognition," in *Proc. IEEE Conf. Comput. Vis. Pattern Recognit. (CVPR)*, Jun. 2016, pp. 5297–5307.

[33] T. Cieslewski, S. Choudhary, and D. Scaramuzza. (2018). *Data-Efficient Decentralized Visual SLAM*. [Online]. Available: https://github.com/uzh-rpg/dslam_open

[34] P. Schmuck, T. Ziegler, M. Karrer, J. Perraudin, and M. Chli, "COVINS: Visual-inertial SLAM for centralized collaboration," in *Proc. IEEE Int. Symp. Mixed Augmented Reality Adjunct (ISMAR-Adjunct)*, Oct. 2021, pp. 171–176.

[35] P. Schmuck, T. Ziegler, M. Karrer, J. Perraudin, and M. Chli. (2021). *COVINS: Visual-Inertial SLAM for Centralized Collaboration*. [Online]. Available: https://github.com/VIS4ROB-lab/covins

[36] L. Bartolomei, M. Karrer, and M. Chli. (2020). *Multi-robot Coordination with Agent-Server Architecture for Autonomous Navigation in Partially Unknown Environments*. [Online]. Available: https://v4rl.ethz.ch/research/datasets-code.html

[37] G. Kim and A. Kim, "Scan context: Egocentric spatial descriptor for place recognition within 3D point cloud map," in *Proc. IEEE/RSJ Int. Conf. Intell. Robots Syst. (IROS)*, Oct. 2018, pp. 4802–4809.

[38] (2021). *DiSCo-SLAM: Distributed Scan Context-Enabled Multi-Robot LiDAR SLAM With Two-Stage Global-Local Graph Optimization*. [Online]. Available: https://github.com/RobustFieldAutonomyLab/DiSCo-SLAM

[39] Y. Chang et al., "LAMP 2.0: A robust multirobot SLAM system for operation in challenging large-scale underground environments," *IEEE Robot. Autom. Lett.*, vol. 7, no. 4, pp. 9175–9182, Oct. 2022.

[40] Y. Chang et al., "LAMP 2.0: A robust multi-robot SLAM system for operation in challenging large-scale underground environments," 2022. [Online]. Available: https://github.com/NeBulaAutonomy/LAMP

[41] P.-Y. Lajoie and G. Beltrame, "Swarm-SLAM: Sparse decentralized collaborative simultaneous localization and mapping framework for multirobot systems," 2023, *arXiv:2301.06230*.

[42] P.-Y. Lajoie and G. Beltrame. (2023). *Swarm-SLAM: Sparse Decentralized Collaborative Simultaneous Localization and Mapping Framework for Multi-Robot Systems*. [Online]. Available: https://github.com/MISTLab/Swarm-SLAM

[43] S. Zhong, Y. Qi, Z. Chen, J. Wu, H. Chen, and M. Liu, "DCL-SLAM: A distributed collaborative LiDAR SLAM framework for a robotic swarm," 2022, *arXiv:2210.11978*.

[44] Y. Wang, Z. Sun, C.-Z. Xu, S. E. Sarma, J. Yang, and H. Kong, "LiDAR iris for loop-closure detection," in *Proc. IEEE/RSJ Int. Conf. Intell. Robots Syst. (IROS)*, Oct. 2020, pp. 5769–5775.

[45] S. Zhong, Y. Qi, Z. Chen, J. Wu, H. Chen, and M. Liu. (2023). *DCL-SLAM: A Distributed Collaborative LiDAR SLAM Framework for a Robotic Swarm*. [Online]. Available: https://github.com/PengYuTeam/DCL-SLAM

[46] C. Cadena et al., "Past, present, and future of simultaneous localization and mapping: Toward the robust-perception age," *IEEE Trans. Robot.*, vol. 32, no. 6, pp. 1309–1332, Dec. 2016.

[47] H. Zhou, Z. Yao, Z. Zhang, P. Liu, and M. Lu, "An online multirobot SLAM system based on LiDAR/UWB fusion," *IEEE Sensors J.*, vol. 22, no. 3, pp. 2530–2542, Feb. 2022.

[48] R. Dubé et al., "SegMap: Segment-based mapping and localization using data-driven descriptors," *Int. J. Robot. Res.*, vol. 39, nos. 2–3, pp. 339–355, Mar. 2020.

[49] P. J. Besl and N. D. McKay, "A method for registration of 3-D shapes," *IEEE Trans. Pattern Anal. Mach. Intell.*, vol. 14, no. 2, pp. 239–256, Feb. 1992.

[50] J. G. Mangelson, D. Dominic, R. M. Eustice, and R. Vasudevan, "Pairwise consistent measurement set maximization for robust multirobot map merging," in *Proc. IEEE Int. Conf. Robot. Autom. (ICRA)*, May 2018, pp. 2916–2923.

[51] G. N. Frederickson, M. S. Hecht, and C. E. Kim, "Approximation algorithms for some routing problems," *SIAM J. Comput.*, vol. 7, no. 2, pp. 178–193, May 1978.

[52] D. Whitley, "A genetic algorithm tutorial," *Statist. Comput.*, vol. 4, no. 2, pp. 65–85, Jun. 1994.

[53] S. Liu, S. J. Liu, N. Harris, and H. M. La, "A genetic algorithm for MinMax K-Chinese postman problem with applications to bridge inspection," in *Proc. Int. Conf. Struct. Health Monit. Intell. Infrastruct.*, 2019, pp. 882–889.

[54] Z. Lu and R. Huang, "Autonomous mobile robot navigation in uncertain dynamic environments based on deep reinforcement learning," in *Proc. IEEE Int. Conf. Real-Time Comput. Robot. (RCAR)*, Jul. 2021, pp. 423–428.

[55] S. Lee, H. Lim, and H. Myung, "Patchwork++: Fast and robust ground segmentation solving partial under-segmentation using 3D point cloud," in *Proc. IEEE/RSJ Int. Conf. Intell. Robots Syst. (IROS)*, Oct. 2022, pp. 13276–13283.

[56] (2021). *EVO: Python Package for the Evaluation of Odometry and SLAM*. [Online]. Available: https://github.com/MichaelGrupp/evo

[57] H. A. Eiselt, M. Gendreau, and G. Laporte, "Arc routing problems—Part I: The Chinese postman problem," *Oper. Res.*, vol. 43, no. 2, pp. 231–242, Apr. 1995.

[58] J. Zhang et al., "Using tabu search to avoid concave obstacles for source location," *IEEE Trans. Intell. Transp. Syst.*, vol. 24, no. 11, pp. 11720–11732, Nov. 2023.

Hongyu Xie (Member, IEEE) received the B.S. degree from Zhengzhou University, Zhengzhou, China, in 2017. She is currently pursuing the Ph.D. degree with the College of Information Science and Technology, Beijing University of Chemical Technology, Beijing, China.

Her research interests include simultaneous localization and mapping and its applications in robotics.

Dong Zhang (Member, IEEE) received the B.S. degree from the University of Jinan, Jinan, China, in 2015, and the Ph.D. degree from the Beijing University of Chemical Technology, Beijing, China, in 2020.

He is currently a Post-Doctoral Fellow with the College of Information Science and Technology, Beijing University of Chemical Technology. His main research interests include design, intelligent control, and optimization of robots.

Xiaobo Hu received the B.S. degree from Chang'an University, Xi'an, China, in 2020. He is currently pursuing the M.S. degree with the Beijing University of Chemical Technology, Beijing, China.

His research interests include SLAM and sensor fusion.

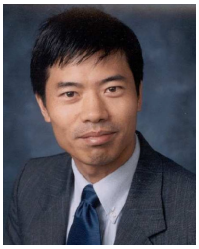

MengChu Zhou (Fellow, IEEE) received the B.S. degree from the Nanjing University of Science and Technology, Nanjing, China, in 1983, the M.S. degree from the Beijing Institute of Technology, Beijing, China, in 1986, and the Ph.D. degree from the Rensselaer Polytechnic Institute, Troy, NY, USA, in 1990.

He joined the New Jersey Institute of Technology (NJIT), Newark, NJ, USA, in 1990, and has been a Distinguished Professor of Electrical and Computer Engineering since 2013. He has over 1100 publications including 14 books, over 750 journal papers (over 600 in IEEE transactions), and 32 book-chapters. He holds 31 patents and several pending ones. His recently co-authored books include *Sustainable Manufacturing Systems: An Energy Perspective*, IEEE Press/Wiley, Hoboken, Hoboken, NJ, 2022 (with L. Li) and *Supervisory Control and Scheduling of Resource Allocation Systems: Reachability Graph Perspective*, IEEE Press/Wiley, Hoboken, NJ, 2020 (with B. Huang). His research interests are in intelligent automation, machine leaning, petri nets, robotics, the Internet of Things, big data, cloud/edge computing, transportation and energy systems.

Dr. Zhou is a Life Member of Chinese Association for Science and Technology-USA and served as its President in 1999. He is a Fellow of International Federation of Automatic Control (IFAC), American Association for the Advancement of Science (AAAS), Chinese Association of Automation (CAA), and National Academy of Inventors (NAI). He is also a member of IEEE TAB Periodicals Committee and Periodicals Review and Advisory Committee. He is a founding Chair/Co-Chair of Technical Committee on AI-based Smart Manufacturing Systems and Technical Committee on Humanized Crowd Computing of IEEE Systems, Man, and Cybernetics Society, Technical Committee on Semiconductor Manufacturing Automation and Technical Committee on Digital Manufacturing and Human-Centered Automation of IEEE Robotics and Automation Society. He is Chair of Fellow Evaluation Committee of Chinese Association of Automation, and a member of Evaluation Committee for both IEEE Systems, Man, and Cybernetics Society and IEEE Robotics and Automation Society. He was General Chair of IEEE Conf. on Automation Science and Engineering, Washington D.C., August 23–26, 2008, General Co-Chair of 2003 IEEE International Conference on System, Man and Cybernetics (SMC), Washington DC, October 5–8, 2003 and 2019 IEEE International Conference on SMC, Bari, Italy, Oct. 6–9, 2019, Founding General Co-Chair of 2004 IEEE Int. Conf. on Networking, Sensing and Control, Taipei, March 21–23, 2004, and General Chair of 2006 IEEE Int. Conf. on Networking, Sensing and Control, Ft. Lauderdale, Florida, U.S.A. April 23–25, 2006. He was Program Chair of 2010 IEEE International Conference on Mechatronics and Automation, August 4–7, 2010, Xi'an, China, 1998 and 2001 IEEE International Conference on SMC and 1997 IEEE International Conference on Emerging Technologies and Factory Automation. He has led or participated in over 60 research and education projects with total budget over $12M, funded by National Science Foundation, Department of Defense, NIST, New Jersey Science and Technology Commission, and industry. He is a recipient of Excellence in Research Prize and Medal from NJIT, Humboldt Research Award for US Senior Scientists from Alexander von Humboldt Foundation, and Franklin V. Taylor Memorial Award and the Norbert Wiener Award from IEEE SMC Society, Computer-Integrated Manufacturing UNIVERSITY-LEAD Award from Society of Manufacturing Engineers, Distinguished Service Award from IEEE Robotics and Automation Society, and Edison Patent Award from the Research and Development Council of New Jersey. He served as an Editor-in-Chief of IEEE/CAA Journal of Automatica Sinica, an Associate Editor of IEEE TRANSACTIONS ON ROBOTICS AND AUTOMATION, IEEE TRANSACTIONS ON AUTOMATION SCIENCE AND ENGINEERING, and IEEE TRANSACTIONS ON INDUSTRIAL INFORMATICS, and an Editor of IEEE TRANSACTIONS ON AUTOMATION SCIENCE AND ENGINEERING. He served as a Guest-Editor for many journals including IEEE INTERNET OF THINGS JOURNAL, IEEE TRANSACTIONS ON INDUSTRIAL ELECTRONICS, and IEEE TRANSACTIONS ON SEMICONDUCTOR MANUFACTURING. He is presently an Associate Editor of Research, IEEE TRANSACTIONS ON INTELLIGENT TRANSPORTATION SYSTEMS, IEEE INTERNET OF THINGS JOURNAL, IEEE TRANSACTIONS ON SYSTEMS, MAN, AND CYBERNETICS: SYSTEMS, AND FRONTIERS OF INFORMATION TECHNOLOGY AND ELECTRONIC ENGINEERING. He has been among most highly cited scholars since 2012 and ranked top one in the field of engineering worldwide in 2012 by Web of Science. He was ranked #99 among the 2023 Top 1000 Scientists in Computer Science in the World, Research.com.

Zhengcai Cao (Senior Member, IEEE) received the B.S. degree in automation from the Heilongjiang University of Science and Technology, Harbin, China, in 1996, and the M.S. degree in electrical engineering and the Ph.D. degree in mechatronic engineering from the Harbin Institute of Technology, Harbin, in 2001 and 2005, respectively.

From 2006 to 2008, he was a Post-Doctoral Researcher with the Research Center of Control Science and Engineering, Tongji University, Shanghai, China. In 2008, he became a Faculty Member of the Beijing University of Chemical Technology, Beijing, China, where he is currently a Professor. From 2014 to 2015, he was a Visiting Scholar with King's College London, London, U.K. His research interests include artificial intelligence and machine learning.